A Brushless Dual-mechanical-port Dual-electrical-port Machine with Spoke Array Magnets in Flux Modulator

Xiang Ren, *Student Member, IEEE*, Dawei Li, *Member, IEEE*, Ronghai Qu, *Senior Member, IEEE* and Tianjie Zou
State Key Laboratory of Advanced Electromagnetic Engineering and Technology,
School of Electrical and Electronic Engineering,
Huazhong University of Science & Technology, Wuhan, China

Brushless dual–mechanical-port dual-electrical-port (BLDD) permanent magnet (PM) machines have been gaining more and more attentions in recent years, with the merits of two decoupled rotors and contactless torque transmission. However, existing BLDD machines tend to suffer from low torque density due to low working flux density. In this paper, a BLDD machine with spoke array permanent magnets (PMs) in flux modular is proposed, which improves the torque density significantly. The structure and operation principle of the proposed machine are introduced. Detailed performance comparison between three different BLDD machine topologies, i.e., surface-mounted PM (SPM) BLDD machine, flux-bidirectional modulation (FBM) BLDD machine, and the proposed BLDD machine, is presented through finite element analysis (FEA). The analyzing results show that although the modulated magnetic field coupled with the modulation winding is slightly reduced, the torque transmission capability of the regular winding in the proposed BLDD machine is significantly enhanced when compared with that of its two counterparts.

***Index Terms*—Brushless dual-mechanical-port dual-electrical-port (BLDD) machine, flux modulation effect, magnetic geared machine (MGM), spoke array permanent magnet**

I. Introduction

As one type of electrical continuously variable transmission (CVT) device, dual-mechanical-port (DMP) machine is widely researched in recent years due to its high compactness, high power density, etc. Owing to these merits, it has great potential in hybrid electrical vehicle (HEV), wind power generation, etc. [1]-[3]. However, brushes and slip rings are used to guide injected current into rotational armature winding in DMP machines, which result in lower reliability and more maintenance.

Based on the flux modulation principle [4]-[6], a new DMP machine type which is named as brushless dual-mechanical-port dual-electrical-port (BLDD) machine was proposed and analyzed, while brushes and slip rings are eliminated and the armature winding is moved to stator. There were different BLDD permanent magnet (PM) machine topologies presented later. In [7] and [8], a BLDD machine which consists of one magnetic geared machine (MGM) and one additional torque regulation machine was proposed, the 2 parts are separated in axial direction. In [9] and [10], two more compact BLDD machine topologies were proposed, where the whole machines are integrated into one frame, while the control strategy was investigated in [11].

Generally, BLDD machines should consist of one MGM part and one PM synchronous machine (PMSM) part, and two torque components, which can be called MGM and PMSM torque component, are produced by two machine parts respectively. The two machine parts can be placed separately in axial direction as in [7] and [8], or integrated into one machine frame as in [9] and [10]. Obviously, the later placement is more compact. However, the PMSM torque component is relatively low considering the magnetic circuit structure, which causes low torque density of the whole BLDD machines.

In this paper, a BLDD machine topology with spoke array magnets in flux modulator is proposed. Due to the special magnetic circuit design, the torque capability of the PMSM part in the proposed machine is increased significantly. In Sec. II, the topology and operation principle of the proposed BLDD machine is introduced. In Sec. III, operation features of the proposed BLDD machine is analyzed, and performance comparison between three different BLDD machine topologies is presented. In Sec. IV, some mechanical issues are discussed. And finally the conclusion is drawn.

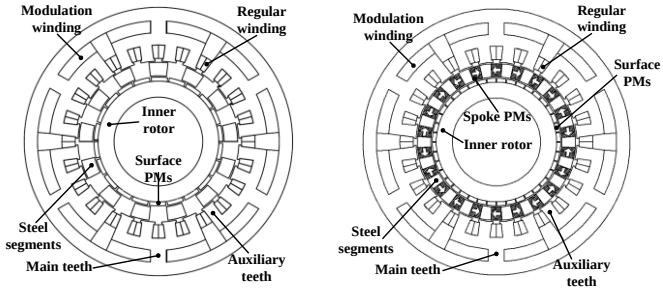

Fig. 1. Cross section. (a) SPM BLDD structure. (b) Proposed BLDD structure.

II. Structure and Operation Principle

A. Structure

The cross sections of SPM and proposed BLDD PM machine topologies are shown in Fig. 1 (a) and (b). Two topologies both have one stator and two coaxial rotors. The special stator configuration is used for both two topologies, i.e., there are auxiliary teeth in the stator. There are two sets of windings, which can be called as modulation winding and regular winding, are placed into main teeth and auxiliary teeth, respectively. This special stator structure provides the two windings more freedom to select slot/pole combinations, which makes it possible to employ non-overlapping winding configuration for both windings. To guarantee the machine performance, the two windings should be decoupled

electrically.

In the SPM BLDD machine shown in Fig. 1(a), the outer rotor is only formed by steel segments (iron pieces), while spoke array PMs are introduced between them in the proposed topology. Further, the pole pair number of modulation winding P_{wr} equals that of spoke PM array P_{ro}, which also differs from that in the SPM BLDD machine, as shown in (1), where P_{ri} is the pole pair number of inner rotor PMs.

$$\begin{aligned} P_{wr} &= P_{ro}\,(\text{for the proposed BLDD machine}) \\ P_{wr} &= P_{ri}\,(\text{for the SPM BLDD machine}) \end{aligned} \tag{1}$$

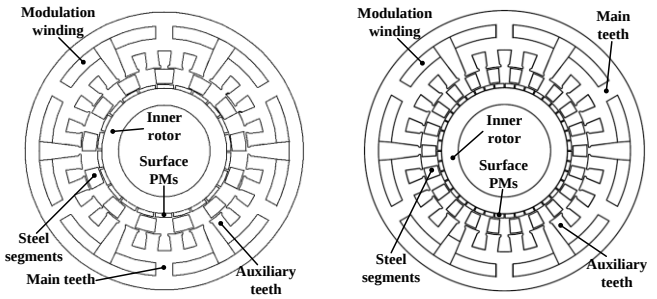

Fig. 2. MGM parts of BLDD machines. (a) SPM BLDD machine. (b) Proposed BLDD machine.

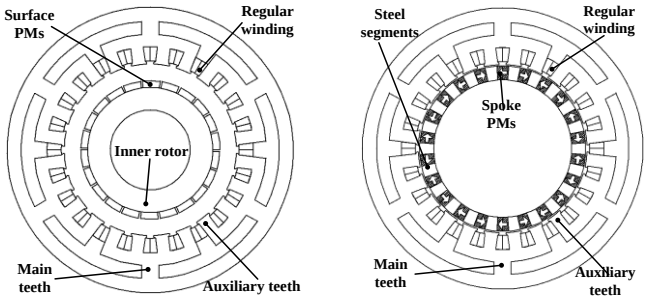

Fig. 3. PMSM parts of BLDD machines. (a) SPM BLDD machine. (b) Proposed BLDD machine.

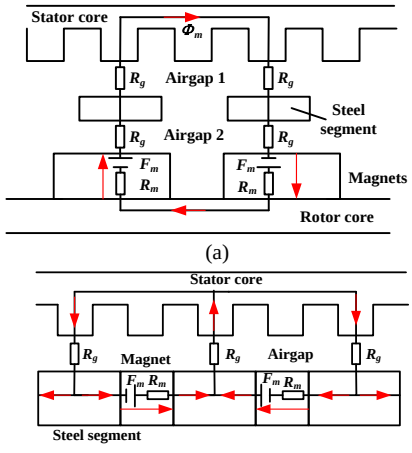

Fig. 4. No load magnetic circuits of PMSM machine parts. (a) SPM BLDD machine. (b) Proposed BLDD machine.

The inner PM rotor is totally the same as that of surface mounted PM rotor, and the pole pair number of modulation winding P_{wm}, surface mounted PMs in inner rotor P_{ri} and number of segment pieces in outer rotor n_{ro} satisfy (2), which is same for the SPM BLDD machine.

$$P_{wm} = n_{ro} - P_{ri} \tag{2}$$

In the proposed BLDD machine, it is obviously that the pole pair number of spoke array magnets in the outer rotor equals half of the number of steel segments, i.e.

$$P_{ro} = \frac{n_{ro}}{2} \tag{3}$$

B. *Operation Principle*

Generally, BLDD machines consist of two machine parts. According to (2), the MGM part is formed by the modulation winding, inner rotor and steel segments in outer rotor, which is same for both SPM and proposed BLDD machines, as shown in Fig. 2. Operation of MGM is based on flux modulation principle, in which steel segments work as a pole pair transformer, and flux density in the airgap can be calculated as (4), where B, F_{ri}, A_{ro}, θ, t, Ω_{ro}, Ω_{ri} represent airgap flux density of MGM part, magnetomotive force produced by inner surface PMs, airgap permeance function, spacial position, time, speeds of outer and inner rotor, respectively, and the airgap permeance function is assumed only consists of constant term Λ_0 and fundamental Λ_1.

$$\begin{aligned} B(\theta,t) &= F_{ri}\Lambda_{ro} \\ &= F_{ri}\cos\left[P_{ri}\left(\theta-\Omega_{ri}t\right)\right]\left\{\Lambda_0+\Lambda_1\cos\left[n_{ro}\left(\theta-\Omega_{ri}t\right)\right]\right\} \\ &= F_{ri}\Lambda_0\cos\left[P_{ri}\left(\theta-\Omega_{ri}t\right)\right] \\ &+\frac{1}{2}F_{ri}\Lambda_1\cos[(n_{ro}\pm P_{ri})\theta-(n_{ro}\Omega_{ro}\pm P_{ri}\Omega_{ri})t] \end{aligned} \tag{4}$$

According to (2) and (4), a P_{wm}-pole-pair field exists in the airgap and it interacts with the modulation winding.

According to (1), PMSM parts of proposed and SPM BLDD machines are technically different. The PMSM part in the proposed BLDD machine is composed of regular winding and outer rotor, while that in the SPM BLDD machine is composed of the regular winding and inner rotor.

As shown in Fig. 4, the magnetic circuit of PMSM machine part in proposed machine is quite different from that in the SPM BLDD machine, where F_m, R_g and R_m are magnetomotive force (MMF) of magnet and reluctance of airgap and magnet respectively. As well known, spoke PM arrangement has benefit of flux focusing effect, and the main magnetic field only passes through one airgap in the proposed BLDD structure, which means lower reluctance and less flux leakage, hence the proposed BLDD machine produces higher P_{wr} pole-pair magnetic field in the outer airgap, and sequentially higher PMSM torque component is produced.

Given the two machine parts mentioned above, torques and speeds of 2 rotors can be controlled by currents in 2 sets of windings, as shown in (5)-(9).

$$T_{ro} = T_{rom} + T_{ror} \tag{5}$$

$$T_{ri} = T_{rim} \tag{6}$$

$$T_{rom} = -\frac{n_{ro}}{P_{ri}}T_{rim} \tag{7}$$

$$P_{ro}\Omega_{ro} = 60\,f_{wr} \tag{8}$$

$$n_{ro}\Omega_{ro} - P_{ri}\Omega_{ri} = 60\,f_{wm} \tag{9}$$

where T_{ro}, T_{rom} and T_{ror} are total, MGM and PMSM torque components on the outer rotor respectively, T_{ri} and T_{rim} are the total and MGM torque components on the inner rotor respectively, f_{wr}, f_{wm} are current frequencies in regular and modulation windings respectively.

III. FEA Study

In order to further investigate principle and performance of the proposed machine, several FEA simulations have been performed. Firstly, the machine operation features, including flux distribution, back EMFs and electromagnetic torque are calculated. Then performances comparison between SPM, FBM and proposed BLDD machine topologies is made.

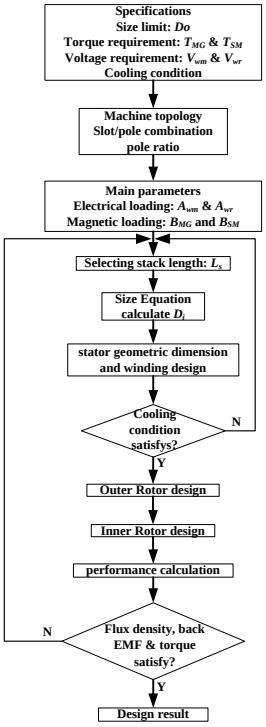

Fig. 5. Initial design process of the proposed BLDD machine.

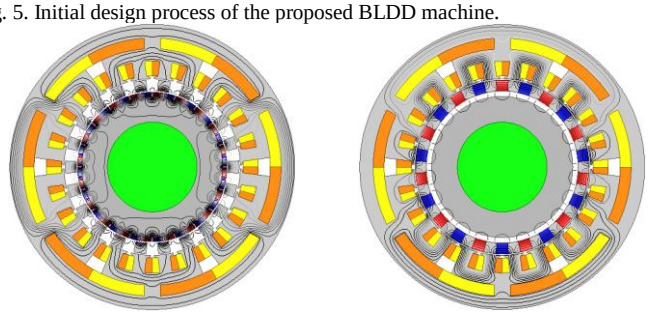

(a) (b)

Fig. 6. Magnetic field distributions excited by PMs at different parts separately. (a) Surface PMs in the inner rotor. (b) Spoke PMs in the outer rotor.

A. Operation Features

A 2-D FEA model is built to calculate the operation features of the proposed machine and verify the principle introduced in Sec. II. The initial design process is illustrated in Fig. 5, where D_o and D_i represent outer and inner diameters of the stator, T_{MG} and T_{SM}, stand for MGM and PMSM torque components, V_{wm}, V_{wr}, A_{wm}, A_{wr} are rated voltage and electrical loading of modulation and regular windings, B_{MG} and B_{SM} denote magnetic loading of the MGM and the PMSM machine parts, respectively. Prior to specific design process, some design indexes, including torque capability, rated voltages and machine outer radius are given. Firstly, rotor pole pair numbers, together with slot/pole combination of two windings are carefully selected. secondly, the electrical and magnetic loadings are practically chosen. The stator inner diameter is then roughly calculated based on the following sizing equations:

$$T_{MG} = \alpha\left(\frac{\sqrt{2}\pi}{4}\right)\left(D_i^2 L_s\right)k_{wm}A_{wm}B_{MG}$$
$$T_{SM} = \left(\frac{\sqrt{2}\pi}{4}\right)\left(D_i^2 L_s\right)k_{wr}A_{wr}B_{SM} \quad (10)$$

where α, k_{wm} and k_{wr} represent pole ratio, winding factors of modulation and regular winding, respectively.

More specific stator and rotor dimensions are designed according to winding cooling condition and flux density restriction After the FEA based design process, some main parameters of the proposed machine are given in Table I.

TABLE I
Main Parameters of SPM and Proposed BLDD Models

Parameters	SPM BLDD	Proposed BLDD
Outer radius of stator/mm	105	
Inner radius of stator/mm	65	
Main teeth number	6	
Auxiliary teeth number	24	
Regular winding pole-pair	11	
Regular winding coil turns	15	
Modulation winding pole-pair	2	
Modulation winding coil turns	84	
Airgap length/mm	1	
Stack length/mm	50	
Steel segment heights/mm	8	4
Inner PMs thicknesses/mm	3	4

Distributions of magnetic fields excited by inner surface and outer spoke PMs separately are shown in Fig. 6. In Fig. 6(a), it can be seen that magnetic fields in stator and inner rotor have different pole pairs, which verifies flux modulation effect in the MGM part. Fig. 6(b) shows the field distribution of PMSM machine part, a 11-pole-pair field is produced in the stator. No load flux density distributions of SPM and proposed BLDD machines are shown in Fig. 7(a) and (b) respectively. Due to excitation of the outer spoke PMs, the proposed BLDD machine produces higher flux density in the stator core, especially in auxiliary teeth.

No load back EMF waveforms of 2 sets of windings at different rotor speeds are shown in Fig. 8. When the outer rotor rotates at 500rpm and the inner rotor is static, period of no load back EMF in the regular winding is 10.91ms, which equals double of that in the modulation winding. When the outer rotor is static and inner rotor rotates, almost no EMF induced in the regular winding. When outer and inner rotor both rotate, periods of EMF in 2 windings differs from that shown in Fig. 8(a). It is noticed that EMF frequencies shown in Fig. 7 matches well with (8) and (9).

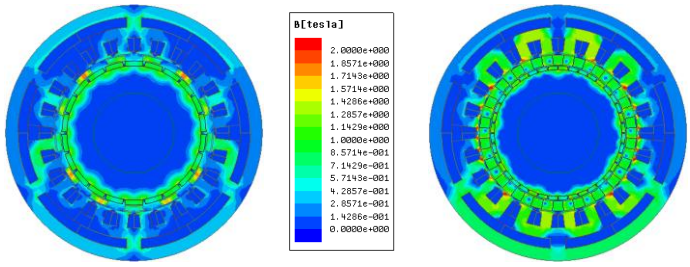

(a) (b)

Fig. 7. No load flux density distributions of BLDD machines. (a) SPM topology. (b) Proposed topology.

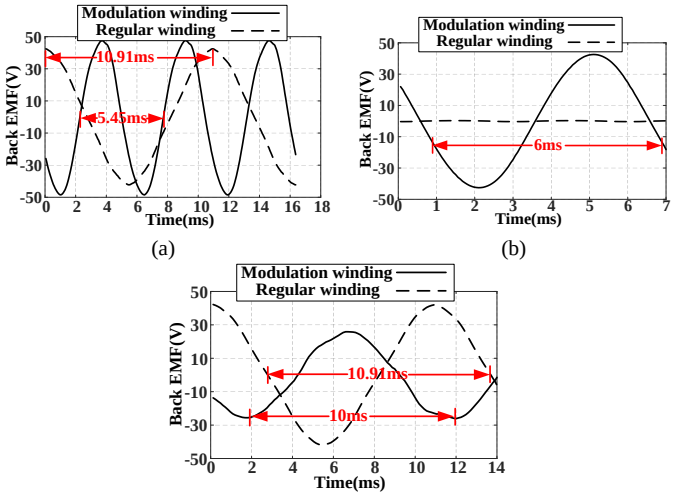

(a) (b) (c)

Fig. 8. Back EMF waveform in different operation conditions. (a) Ω_{ro}=500rpm, Ω_{ri}=0. (b) Ω_{ro}=0, Ω_{ri}=500rpm. (c) Ω_{ro}=500rpm, Ω_{ri}=250rpm.

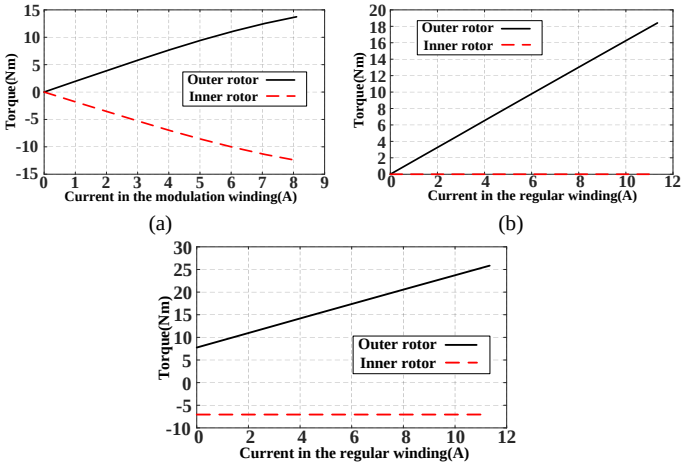

(a) (b) (c)

Fig. 9. Electromagnetic torques on 2 rotors at different operation conditions. (a) I_{wr}=0. (b) I_{wm}=0. (c) I_{wm}=4.05A.

output torque characteristics of the proposed machine at different operation conditions are presented in Fig. 9. When the regular winding is at open circuit, only MGM torque component acts on 2 rotors. As shown in Fig. 9 (a), T_{ro} and T_{ri} are proportional to I_{wm}, which matches well with (7). When the modulation winding is at open circuit, only the PMSM torque component works on the outer rotor, which means T_{ri} equals zero and T_{ro} is proportional to I_{wr}, as shown in Fig. 9 (b). In Fig. 9 (c), I_{wm} is constant and I_{wr} varies, which means T_{ri} and T_{rom} are constant and T_{ror} varies linearly with the increase of I_{wr}.

B. Performance Comparison

A SPM BLDD machine as shown in Fig. 1(a) is designed for performance comparison. Its main parameters are given in Table I, which have been optimized for higher torque production. Compared with the proposed machine, it has same stator but different rotor topology and sizes.

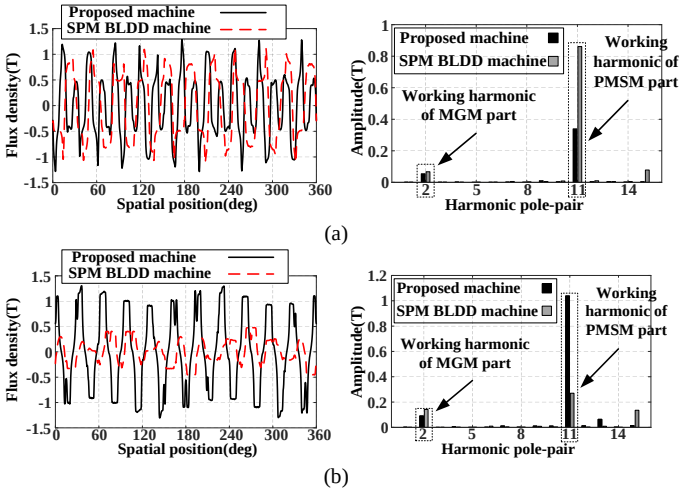

(a) (b)

Fig. 10. Magnetic fields and spectrums in airgaps. (a) Inner gap. (b) Outer gap.

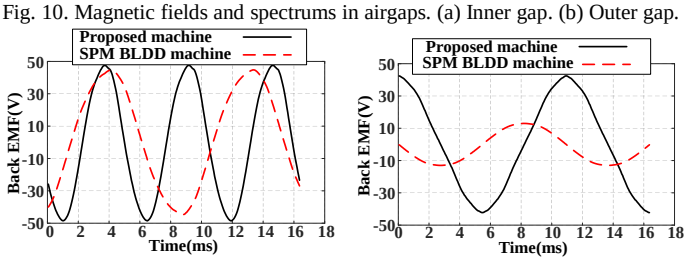

(a) (b)

Fig. 11. No-load back EMF comparison of the SPM and proposed BLDD machines. (a) Modulation winding. (b) Regular winding.

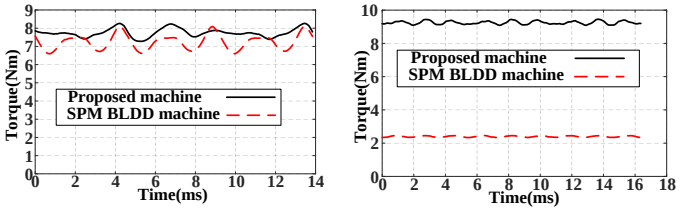

(a) (b)

Fig. 12 Torque components comparison between SPM and proposed BLDD machines. (a) MGM torque component. (b) PMSM torque component.

Flux density waveforms and spectrums of SPM and proposed BLDD machines in inner and outer airgaps are shown in Fig. 10 (a) and (b) respectively. The 11-pole-pair field of the SPM BLDD machine reaches 0.85T in the inner gap, however, due to flux modulation effect and flux leakage, only 0.27T remains in the outer gap, which equals about 1/4 of that in the proposed BLDD machine, and this result verifies the analysis of magnetic circuits in Sec. II.

Fig. 11 (a) shows no load back EMFs in modulation winding of 2 models when their outer rotors both rotate at 500rpm. Although the 2-pole-pair field in the outer gap of the proposed BLDD machine is lower than that of the SPM BLDD machine, the proposed machine has a higher gear ratio, hence a higher back EMF value is obtained. Fig. 11 (b) shows

back EMF comparison in regular windings, EMF of the proposed BLDD machine is about 4 times that of the SPM BLDD machine, which matches well the analysis of magnetic fields.

Output torque comparison between SPM and proposed BLDD machine is shown in Fig. 12, I_{wr} and I_{wm} are 4.05A and 5.67A respectively for both models. the MGM torque component increases by about 7%, and the PMSM torque component increases to about 4 times in the proposed BLDD machine. Considering magnet material usage, the MGM torque component per unit magnet usage in the proposed machine is about 57.2% of the SPM BLDD machine, while this value is 224.7% for the PMSM torque component.

In order to further illustrate features of the proposed BLDD machine, another comparison with BFM BLDD machine [10] is made. Parameters and sizes of two models are shown in Table II. For a convictive comparison, the outer and inner radius, stack length, turns in series per phase and pole ratio are kept the same for both machine models.

TABLE II
PARAMETERS OF BFM AND PROPOSED BLDD MACHINES

Parameters	BFM BLDD[10]	Proposed BLDD
Outer radius of stator/mm	108	
Inner radius of stator/mm	74.4	
Slot number	48	24
Regular winding pole-pair	28	14
Regular winding coil turns	23	46
Modulation winding pole-pair	11	
Modulation winding coil turns	23	46
Airgap length/mm	1	
Stack length/mm	50	
Outer rotor heights/mm	6.1	8
Inner PMs thicknesses/mm	15.8	3
Rotation speed/rpm	500	500
Input current/A	4.72	4.72

TABLE III
PERFORMANCES OF BFM AND PROPOSED BLDD MACHINES

Parameters	BFM BLDD	Proposed BLDD
Modulation winding no load back EMFs/V	30.2	29.3
Regular winding no load back EMFs/V	49.2	72.8
MGM torque components/Nm	6	5.4
PMSM torque components/Nm	9.6	13.9
MGM torque per kg magnet/Nm/kg	3.8	5.5
PMSM torque per kg magnet/Nm/kg	6.1	14.2

Table III summarizes the results, and shows that although the proposed BLDD machine produces ~3% lower fundamental back-EMF in the modulation winding and 10% lower MGM torque than that of the BFM BLDD machine, the back-EMF in the regular winding and the PMSM torque component are ~48% and ~45% higher. Moreover, the magnet material consumption of the proposed machine is only 62% that of the BFM BLDD machine, and a more competitive value of torque per unit magnet usage is achieved accordingly.

Furthermore, since the slot number for the regular and modulator windings can be independent selected in the proposed machine due to its special stator configuration, the non-overlapping winding configuration can be used for both the two windings to reduce the end winding length. This means that the proposed machine can operate at a higher electric loading to enlarge the output torque.

IV. MECHANICAL ISSUES

In this section, the mechanical structure of the proposed BLDD machine is presented. The mechanical stress and its influence on electromagnetic performances are evaluated.

Fig. 13. 3D structure of the outer rotor

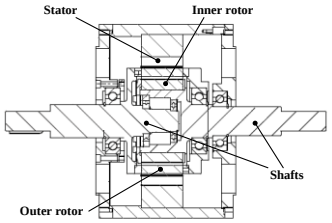

Fig. 14. Assembly graph of the proposed machine.

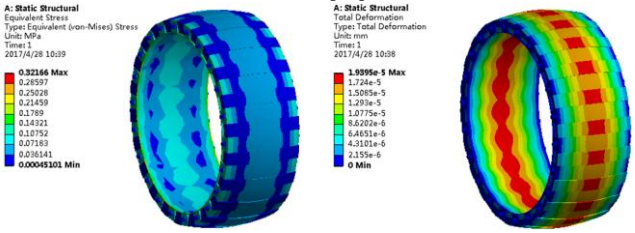

Fig. 15. Mechanical stress analysis of the outer rotor.

The 3D structure of the outer rotor is shown in Fig. 13. A 0.5mm magnetic bridge is added at the bottom of steel segments, trapezoid magnets are adopted to mounted between segments, and mounting holes are punched at the center of each segment. The assembly graph of the whole machine is shown in Fig. 14, in which both the two rotors are with robust mechanical structure, i.e. two-side support .

The mechanical stress of the outer rotor at 500rpm is checked, as shown in Fig. 15. The maximum mechanical stress of the rotor support is 0.32MPa, which is much smaller than the yield strength of the carbon steel. The influence of the magnetic bridge and mounting holes on electromagnetic performance of the proposed machine are summarized in Table IV. The MGM and PMSM torque components are ~9% and ~10% reduced, respectively considering these mechanical structures.

TABLE IV
ELECTROMAGNETIC PERFORMANCE COMPARISON BETWEEN BLDD MACHINES WITH AND WITHOUT MECHANICAL STRUCTURES

Parameters	Without mechanical structures	With mechanical structures
Modulation winding no load back EMFs/V	35.1	30.2
Regular winding no load back EMFs/V	44.2	40.3
MGM torque components/Nm	7.8	7.1
PMSM torque components/Nm	9.1	8.2

V. CONCLUSION

In this paper, a BLDD machine with spoke array magnets in flux modular has been proposed, while spoke array magnet rotor structure is employed to work as flux source of the

PMSM part and flux modulator of the MGM part at the same time. With flux-focusing effect utilized and magnetic resistance of the PMSM part decreased, the working flux density and corresponding PMSM torque component are much higher.

Furthermore, decoupled control of speeds and torques of the proposed BLDD machine has been verified through FEA, Then, the proposed BLDD machine has been compared with existing SPM and BFM BLDD machine topologies on electromagnetic performance. The analysis results show that the PMSM torque component of the proposed machine are ~300% and ~45% higher compared with those of the SPM and BFM BLDD machine, respectively. Finally, an outer rotor structure with magnetic bridge and mounting holes is further proposed for the consideration of practical fabrication. Reliable mechanical support of the outer rotor has been verified though mechanical stress evaluation.

REFERENCES

[1] S. Eriksson and C. Sadarangani, "A four-quadrant HEV drive system," in *Proc. IEEE 56th Veh. Technol. Conf*., 2002, pp. 1510–1514.
[2] M. J. Hoeijmakers and J. A. Ferreira, "The electric variable transmission," *IEEE Trans. Ind. Appl.*, vol. 42, no. 4, pp. 1092-1100, July-Aug. 2006.
[3] L. Xu, "A new breed of electrical machines-basic analysis and applications of dual mechanical port electric machines," in *Proc. 8th Int. Conf. Elect. Mach. Syst*., Nanjing, China, 2005, vol. 1, pp. 24–31.
[4] L. L. Wang, J. X. Shen, P. C. K. Luk, W. Z. Fei, C. F. Wang and H. Hao, "Development of a Magnetic-Geared Permanent-Magnet Brushless Motor," *IEEE. Trans. Magn*., vol. 45, no. 10, pp. 4578-4581, Oct. 2009.
[5] C. Liu, K. T. Chau and Z. Zhang, "Novel design of double-stator single-rotor magnetic-geared machines," *IEEE Trans. Magn*., vol. 48, no. 11, pp. 4180-4183, Nov. 2012.
[6] Padmanathan, P.; Bird, J.Z. "A continuously variable magnetic gear", *in Proc. IEEE IEMDC*, 2013, pp:367-373.
[7] P. Zheng, J.G. Bai, C.D. Tong, Y. Sui, Z.Y Song, and Q.B Zhao, "Investigation of a novel radial magnetic-field-modulated brushless Double-rotor machine used for HEVs," *IEEE Trans. Magn.*, vol. 49, no. 3, pp. 1231-1241, Mar. 2013.
[8] J. Bai, P. Zheng, C. Tong, Z. Song and Q. Zhao, "Characteristic analysis and verification of the magnetic-field-modulated brushless double-rotor machine," *IEEE Trans. Ind. Electron*., vol. 62, no. 7, pp. 4023-4033, July 2015.
[9] D. Li, R. Qu, X. Ren and Y. Gao, "Brushless dual-electrical-port, dual mechanical port machines based on the flux modulation principle," in *Proc. IEEE Energy Convers. Congr. Expo*,2016.
[10] Y. Liu, S. Niu and W. Fu, "Design of an electrical continuously variable transmission based wind energy conversion system," *IEEE Trans. Ind. Electron*., vol. 63, no. 11, pp. 6745-6755, Nov. 2016.
[11] X. Luo; S. Niu, "A novel contra-rotating power split transmission system for wind power generation and its dual MPPT control strategy," *IEEE Trans. Power Electron.*, accepted.